

https://dspace.org/

Properties of weakly cemented slurries of gold mine slimes

Avalle, Derek Luigi

2014-10-15
http://hdl.handle.net/10539/15745

Downloaded from a DSpace repository. https://dspace.org/

3 SHEAR STRENGTH PROPERTIES

3.1 The Triaxial Test

The triaxial compression test was used to provide information on the shear properties of the material[11]. Each 38 mm cylindrical specimen, approximately 76 mm in length, was sheathed in an impermeable rubber membrane and placed in the triaxial cell[11]. A lateral stress was applied by controlling the water pressure on the rubber membrane, and the axial stress was applied by a loading piston through the upper capped end of the specimen. The specimen was loaded at a constant rate of strain until failure. The stress data can be plotted in terms of Mohr circles, from which shear strength envelopes can be derived.

In the triaxial tests reported here, specimens were isotropically consolidated under the desired cell pressure and with no back pressure. During this process the coefficient of consolidation was measured by recording the rate of change of volume with time.

Two types of tests were conducted on the isotropically consolidated specimens:

a) the undrained test: the apparatus was equipped with a device for maintaining the specimen at a constant volume, thus enabling pore water pressure to be measured during loading, and

b) the drained test: the specimen was allowed to drain freely during loading, the amount of drainage being measured by the volume change apparatus.

If σ is the total stress on the specimen and u is the pore water pressure in the specimen, then the effective stress, σ', is defined as:

$$\sigma' = \sigma - u$$

Effective stresses can thus be calculated from the information recorded in the undrained tests, but it can be seen that with free drainage in the drained tests, u = o, and the total stresses measured are thus equal to effective stresses.

3.2 Typical Results

The coefficient of consolidation*, c_v, was calculated during each isotropic consolidation by plotting volume decreases against the square root of time in minutes. The drainage was from one end only, and the c_v for this case is given by [11]:

$$c_v = \frac{\pi h^2}{t_{100}}$$

where 2h = height of sample, and $\sqrt{t_{100}}$ is defined by the point on the curve given by the intersection between the extrapolated initial straight portion of the curve and the line representing 100% consolidation. Fig. 12 shows a typical curve and calculation of c_v.

* the coefficient of consolidation is the constant of proportionality in the differential equation of consolidation

$$\frac{\partial u}{\partial t} = c_v \frac{\partial^2 u}{\partial Z^2}$$

The c_v is thus a measure of the rate of unsteady flow of water through a soil and is a function of the permeability, void ratio and compressibility of the soil.

K. Terzaghi. Theoretical Soil Mechanics, p.271

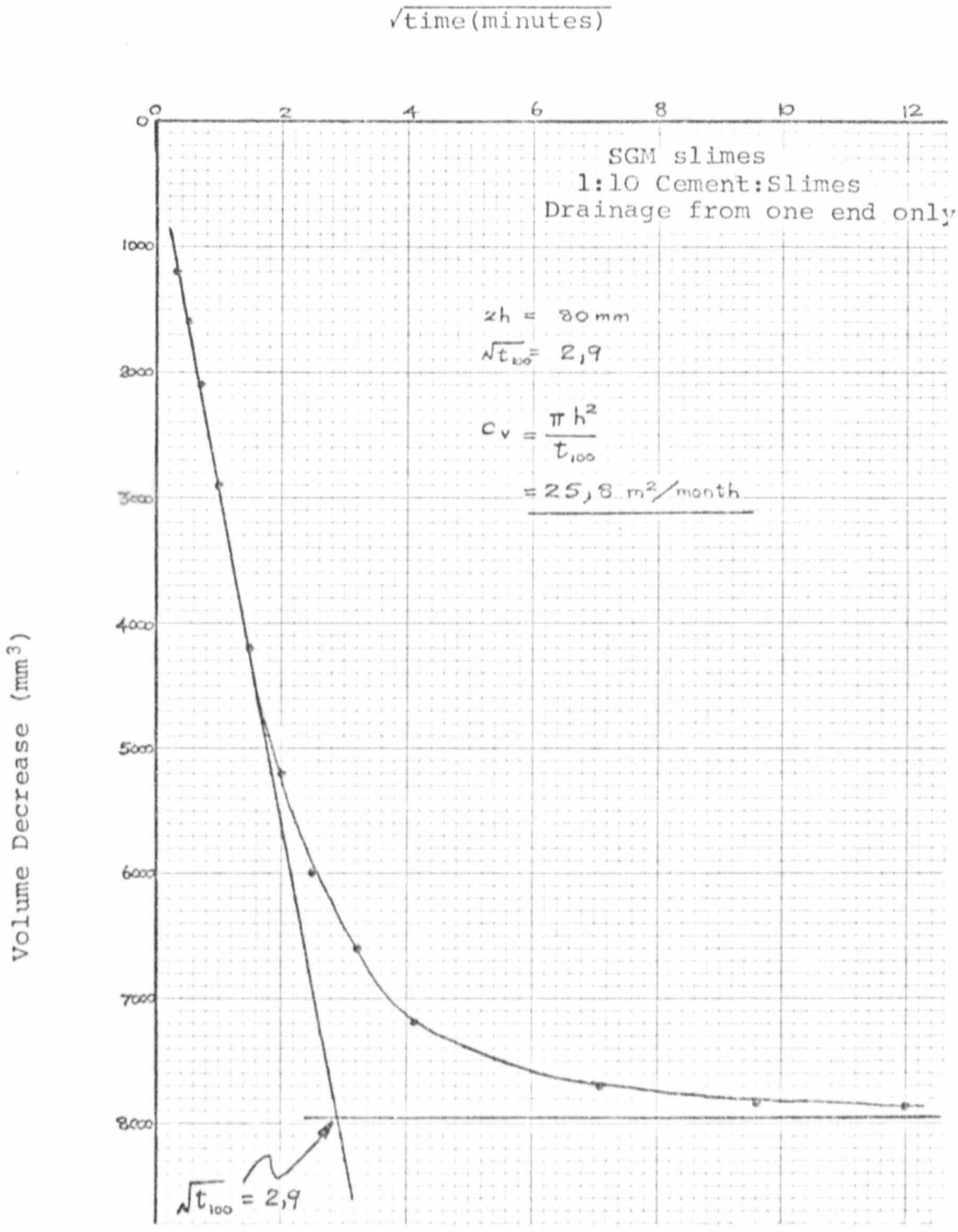


Fig. 12 Typical Curve and Calculation for Coefficient of Consolidation

The results of a typical set of drained and undrained triaxial tests are shown in Figs. 13 and 14 for SGM and ROD slimes respectively. The stress-strain curves are plots of the vertical or deviator stress, $(\sigma_1-\sigma_3)$, versus the axial strain, the stresses and strains being calculated directly from readings of load and deflection taken during the tests. The largest recorded stress is taken as the failure stress of the material at the particular lateral stress.

During the undrained tests, pore water pressures were measured. The pore water pressure in the ROD slimes sample (Fig. 14b) drops before failure and more sharply than in the SGM slimes (Fig. 13b). This indicates that the ROD slimes was denser and dilated more strongly, which is also apparent in the volume change curves plotted from drained test data. The fact that the ROD slimes dilates more strongly than the SGM slimes indicates that the ROD slimes should be less susceptible to liquefaction than the SGM slimes. Volume increase and pore pressure decrease both act in favour of reducing the possibility of liquefaction[8].

3.3 Coefficients of Consolidation

The range of measured c_v values are tabulated below. For comparison, Blight[12] reported an average c_v of about 31 m^2/month (4000 sq.ft/year) for a slimes material similar in properties to SGM slimes.

Type of slimes	Additives	Range of c_v (m^2/month)
SGM	Cement, cement-flyash	20-27
SGM	Lime-flyash gypsum-lime-flyash	28-35
ROD	Cement	10-18

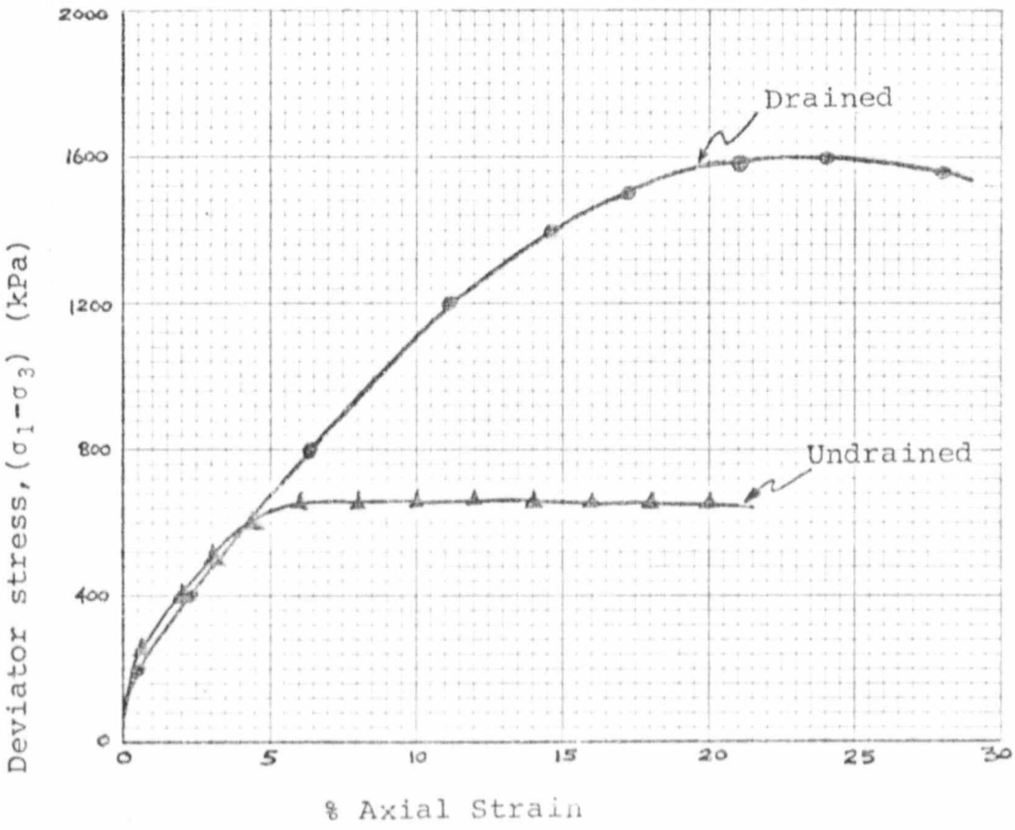


Fig. 13a Stress-Strain Curves

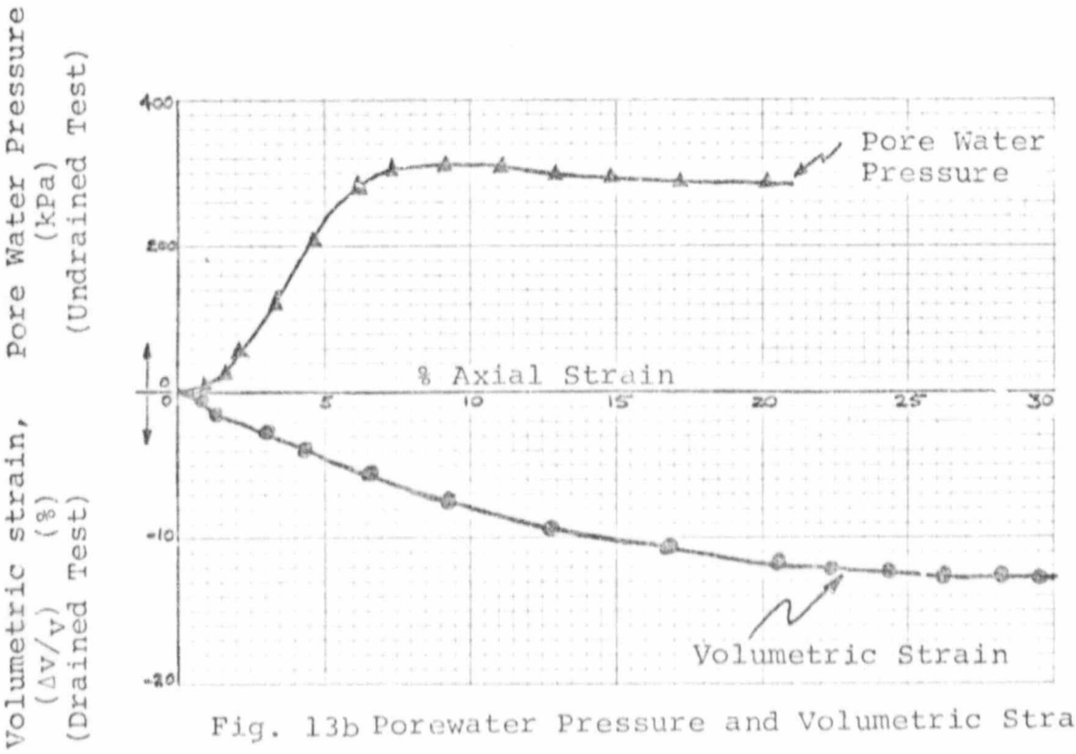


Fig. 13b Porewater Pressure and Volumetric Strain Curves

Fig. 13 Typical Curves for Drained and Undrained Triaxial Tests on SGM slimes

(1:10 Cement:Slimes, 7-10 days Curing, Cell Pressure = 493 kPa)

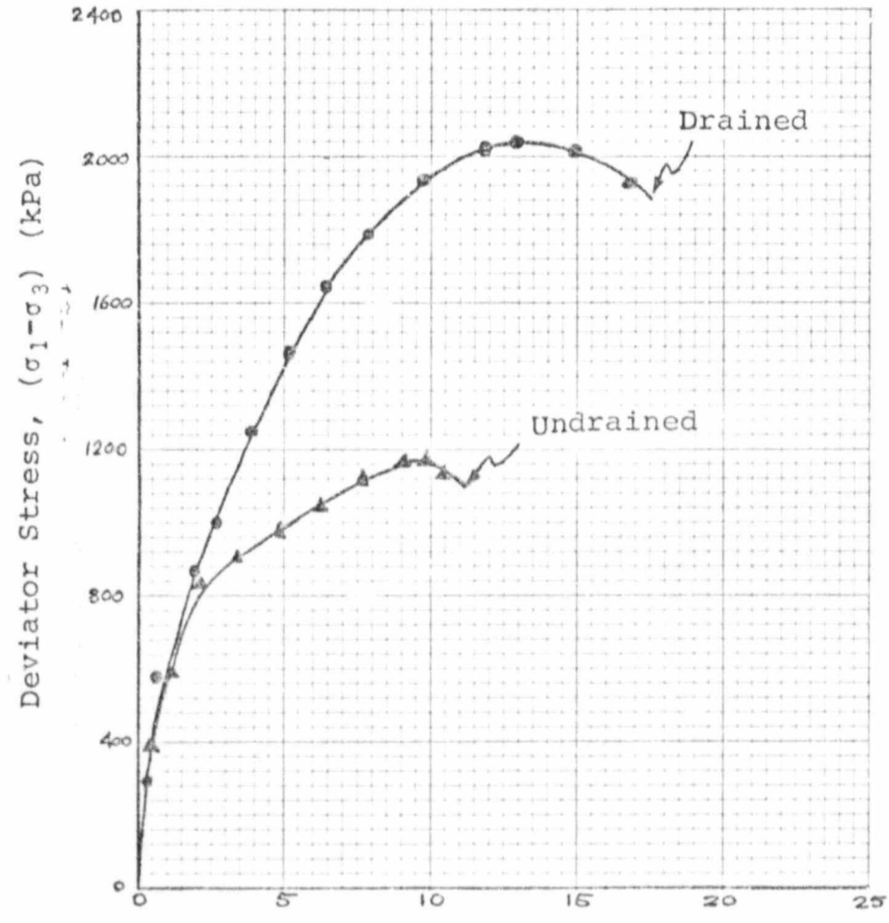


Fig. 14a Stress-strain curves

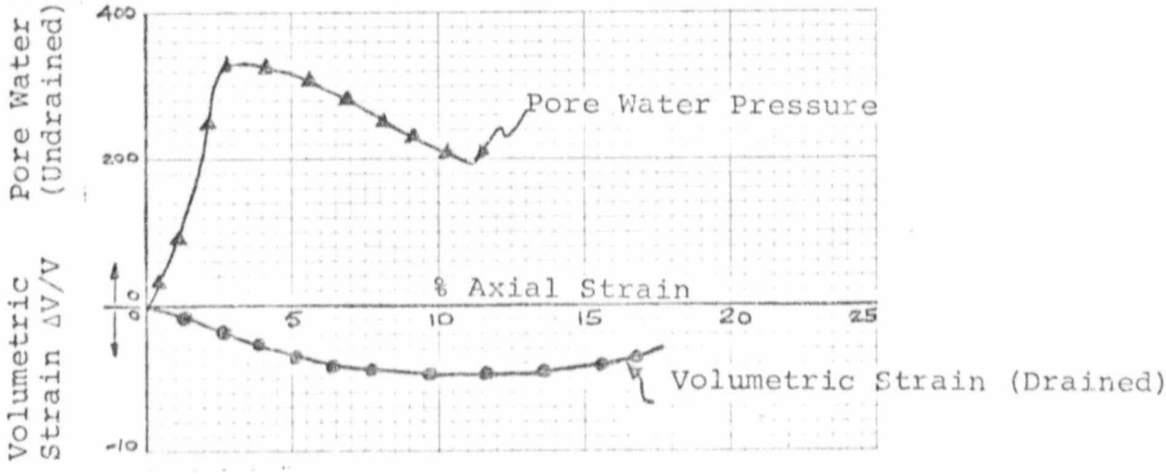


Fig. 14b Pore water pressure and volumetric strain curves.

Fig. 14 Typical Curves for Drained and Undrained Triaxial Tests on ROD slimes
(1:10 Cement:slimes, 7-11 days Curing, Cell Pressure = 493 kPa)

3.1 Shear Strength Envelopes

Each drained shear strength envelope shown in Fig. 15 was plotted using the results of at least three undrained triaxial tests conducted at different cell pressures. If the minor principal or radial stress is σ_3, then the failure stress in the triaxial test is the deviator stress, $(\sigma_1-\sigma_3)$, where σ_1 is the major principal or axial stress. Half of the deviator stress, $\frac{1}{2}(\sigma_1-\sigma_3)$, is the radius of the Mohr circle, the centre of which lies at $\frac{1}{2}(\sigma_1+\sigma_3)$. Since the pore pressure was zero in all drained tests of this program, the effective stresses were equal to the applied stresses, and each shear strength envelope in terms of effective stress was obtained directly from the total stress Mohr circles at failure. A line tangential to all the circles forms the shear strength envelope. The cohesion, c, is the intercept of the envelope on the vertical axis, and the angle of shearing resistance, ϕ, is the slope of the envelope.

Fig. 15 shows the shear strength envelopes in terms of effective stress for mixtures of SGM slimes with various additives, and for ROD slimes with cement.

The low cohesion value of the material is explained by the low additive content of the mixes. Trends in the angle of shearing resistance indicate that the most favourable additive combination is that of cement and flyash (Fig. 15a). The coarser nature of the ROD slimes is again shown up by the steeper shear strength envelope (Fig. 15c).

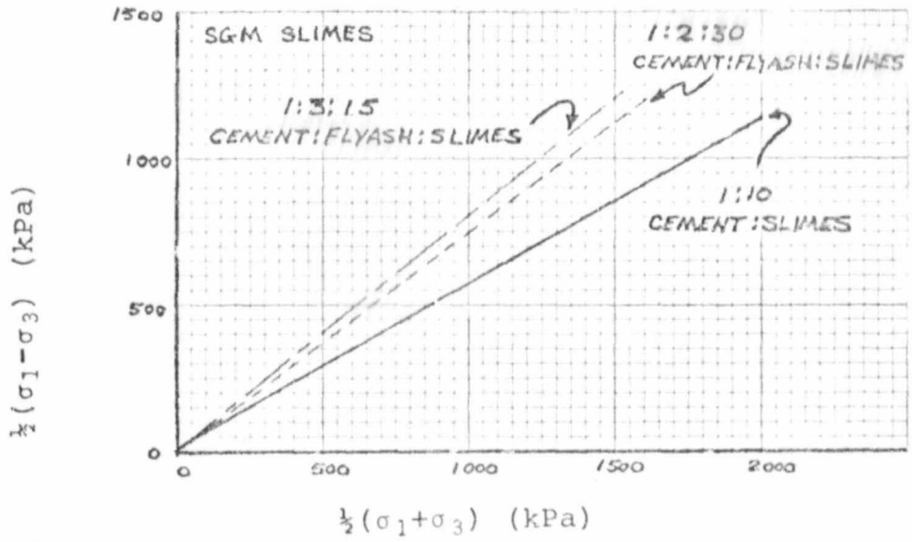


Fig. 15a SGM slimes with cement and cement-flyash

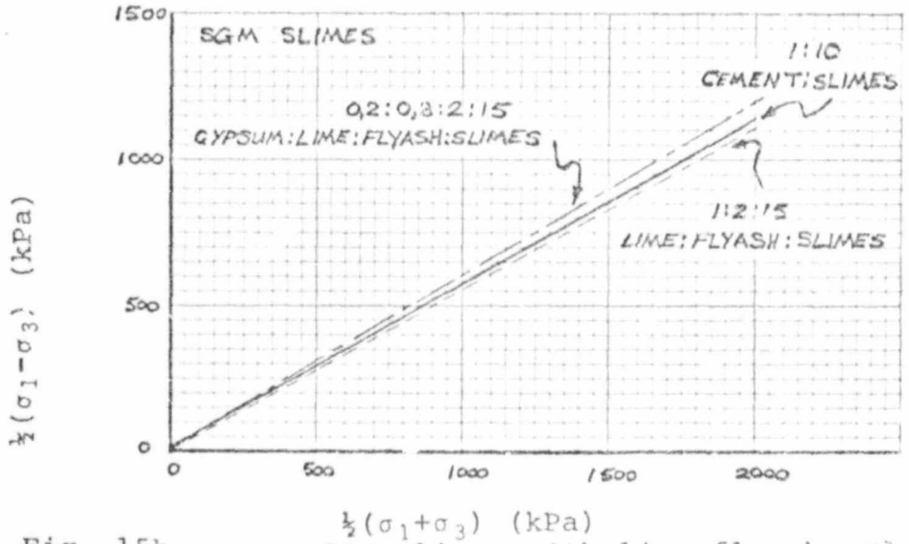


Fig. 15b SGM slimes with lime-flyash and gypsum-lime-flyash

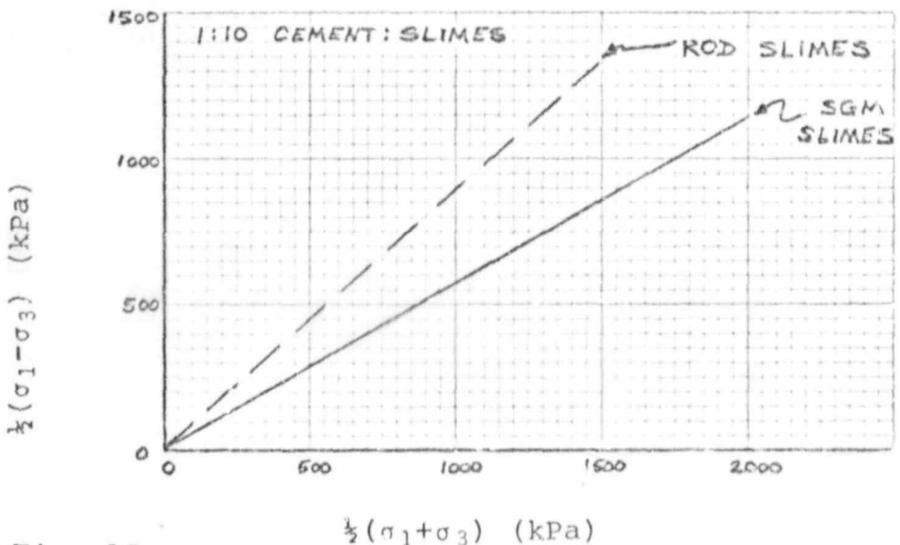


Fig. 15c SGM and ROD slimes with cement

Fig. 15 Shear strength Envelopes

4. STRENGTH DEVELOPMENT UNDER LOAD

4.1 Testing Techniques

The strength development of stabilised slimes under laod was measured by means of compression tests on slab specimens which were intended to model conditions in an hydraulically filled stope. Load and vertical strain were recorded for each test. Results are presented as plots of calculated vertical stress (load/area) versus vertical strain or percentage closure.

A standard curing period of 7 days was aimed at, but curing times in excess of 7 days were found to have little effect on the results. A testing time of about 45 minutes was chosen, after tests of over 6 hours duration showed insignificant variations in results from the faster tests.

Plan dimensions of the slabs were varied (varying the height:shorter side ratio) and this was found to have very little effect on stress-strain curves for similar mixes. In particular, two tests on 30 mm high slabs of SGM slimes with 1:10 cement:slimes, one a 150x90 mm slab (height:shorter side ratio 1:3), the other 180x180 mm (height:side ratio 1:6), resulted in almost identical stress-strain curves.

Filter paper drains both above and below the slabs were used in all tests except those on mould-restrained specimens. In these latter tests, 20 mm thick mild steel platens just fitting into the moulds were used to transfer the load onto the specimens, and a paper drain was provided at the bottom of the specimens only. The purpose of providing filter paper drains was to simulate in the model slab specimens the conditions of drainage, through cracks and fissures in the rock, that exist during in mine stopes.

4.2 Unreinforced Slabs

In the tests on unreinforced slabs, no restraint was applied to lateral movement. The slabs were compressed between wide platens and the plan dimensions of the slabs increased during the tests. Measurements of the sides were taken before and after each test, and in order to calculate the stresses, a straight line variation was assumed between the closure strain and the ratio of loaded area to initial area. This relationship was used to correct stresses calculated on the basis of the initial area.

Fig. 16 shows the results of tests on unreinforced slabs of SGM slimes stabilised with cement and cement-flyash. All mixes were initially at 54% moisture content. The marked improvement shown by the 1:2:15 cement:flyash:slimes mix over the 1:10 cement:slimes mix indicates that the use of flyash with cement can be beneficial to the strength development characteristics while utilising a lesser proportion of cement. Cement-flyash-slimes mixes with lower proportions of cement produced results of a less favourable nature, as has been observed overseas[5].

The effects of lime-flyash and gypsum-lime-flyash as additives to SGM slimes are shown in Fig. 17. The improvement gained from the addition of small amounts of gypsum supports previous research[7]. The 1:2:15 lime:flyash:slimes mix is slightly weaker than the 1:10 cement:slimes mix (Fig.17), and is substantially weaker than the 1:2:15 cement:flyash:slimes mix (Fig.16). However the inclusion of gypsum for between 10% and 30% of the lime results in strength development curves comparable with the 1:10 cement:slimes mix (Fig. 17).

1:10 cement:slimes

1:2:30

1:3:30

1:2:15

1:3:15

Lime:Flyash:Slimes

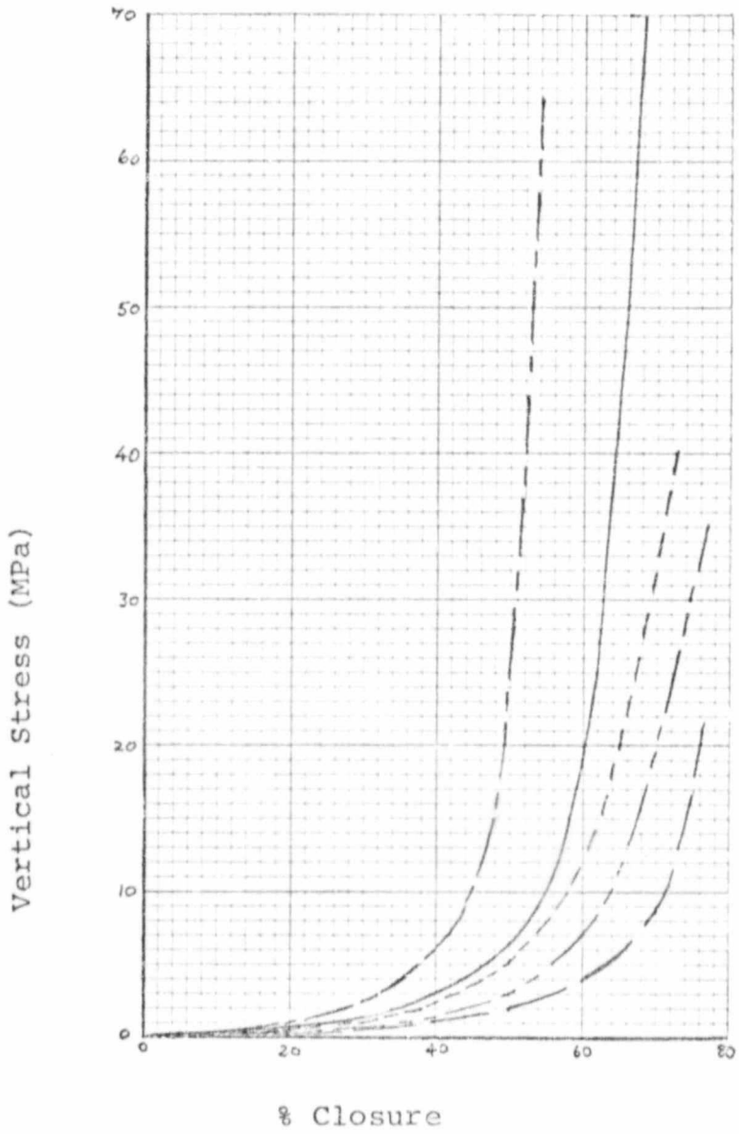
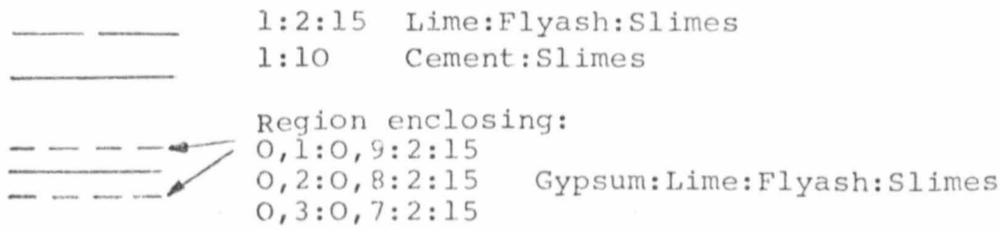


Fig. 16 Stress-strain Curves for SGM slimes with Cement and Cement-Flyash



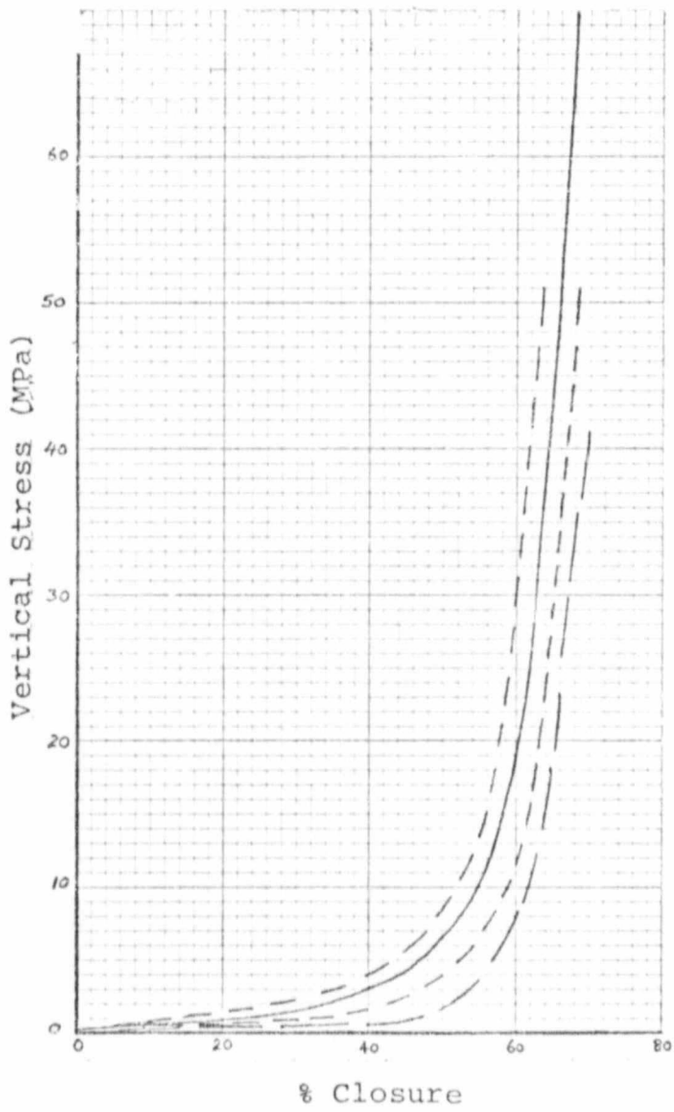


Fig. 17 Stress-Strain Curves for SGM Slimes with Cement, Lime-Flyash and Gypsum-Lime-Flyash

Fig. 18 shows the results of a test on a slab of ROD slimes with 1:10 cement:slimes and 35% moisture content. The pronounced improvement in strength development shown by the slab of ROD slimes compared with a similar slab of SGM slimes is considered to be due to the better shear properties (see Fig. 15c)as well as the lower initial moisture content.

To test the effect of initial moisture content on strength development,slab tests were conducted on two mixes of cement and SGM slimes with 1:8 and 1:15 cement: slimes ratios, both cast with initially 40% moisture content. The results, shown in Fig. 19, indicate the importance of initial moisture content with regard to strength development. Even the leaner 1:15 cement: slimes mix cast at 40% moisture content is seen to give improved results over the 1:10 mix cast at 54% moisture content. It must therefore be emphasized that the denser the slurry that can be pumped, the better will be its strength development characteristics under load.

Immediately after the tests on SGM slimes mixes, profiles of moisture content across a central axis of the slabs were obtained. Fig. 20 shows a typical moisture content profile across a slab after loading to about 70 MPa. The moisture content at the centre of the slabs varied between 6% and 9% after testing. The edges of the slabs crumbled and free water was squeezed out of the slabs during the tests.

4.3 Wire-reinforced Slabs

In this series of tests, reinforcement consisting of 1,65 mm diameter annealed binding wire was placed at mid-depth in the slab moulds before casting. Apart from the reinforcing wires, no restraint was applied to lateral movement of the slabs during testing. As with the unreinforced slabs, the plan dimensions of the wire-reinforced slabs increased with compression, but generally not as much as in the unreinforced case.

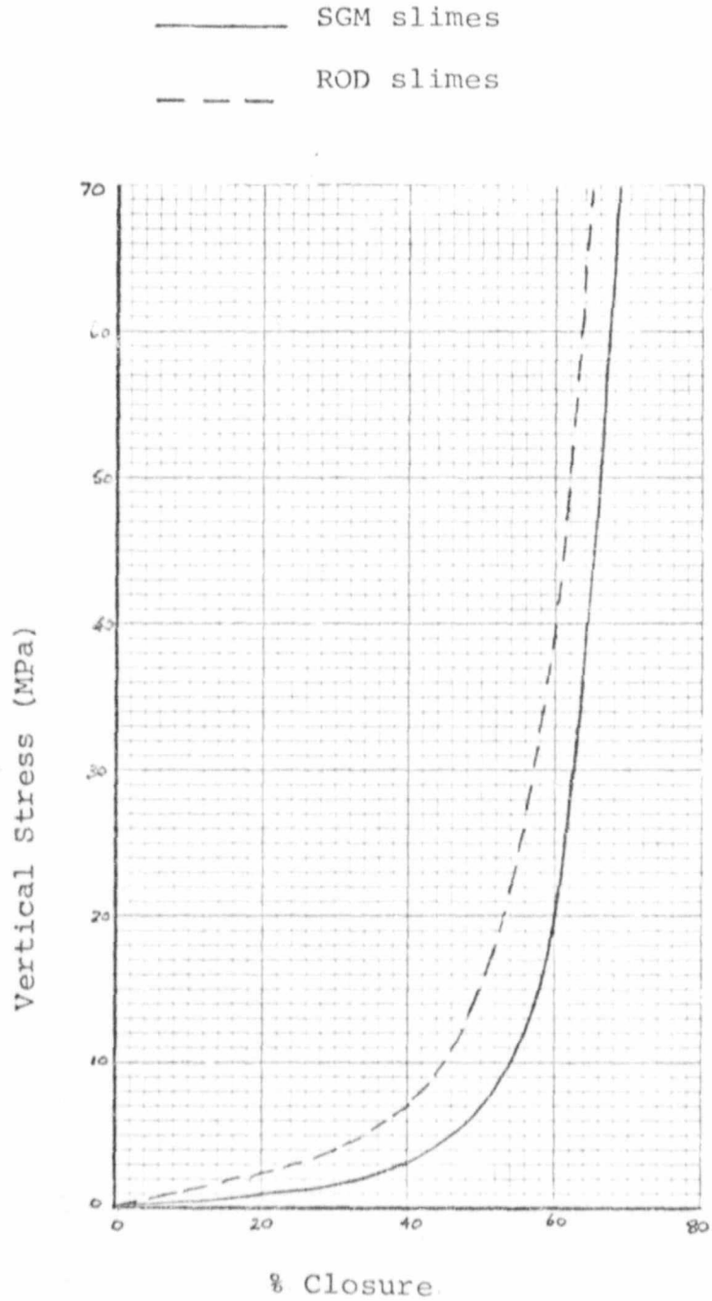


Fig. 18 Stress-Strain Curves for SGM and ROD slimes with Cement (1:10 Cement:Slimes Ratio)

	Cement:Slimes Ratio	% Moisture Content
———	1:10	54
– – – –	1:15	40
—— ——	1:8	40

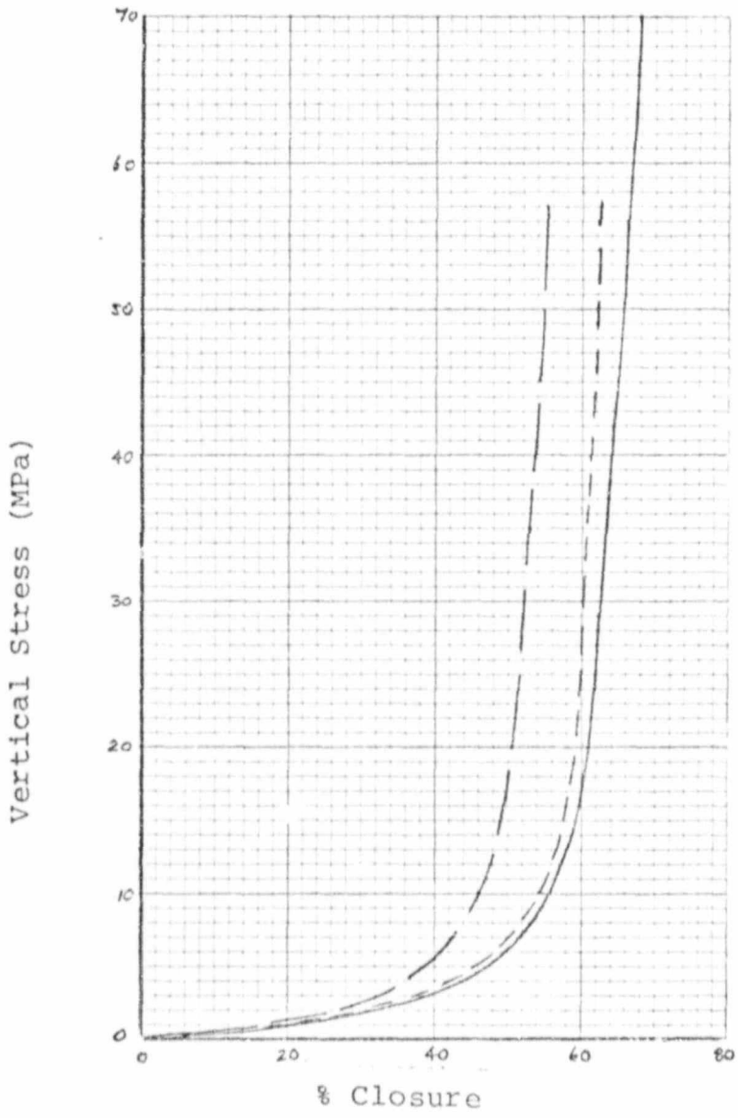


Fig. 19 Effect of Moisture Content Reduction on Strength Development (SGM Slimes)

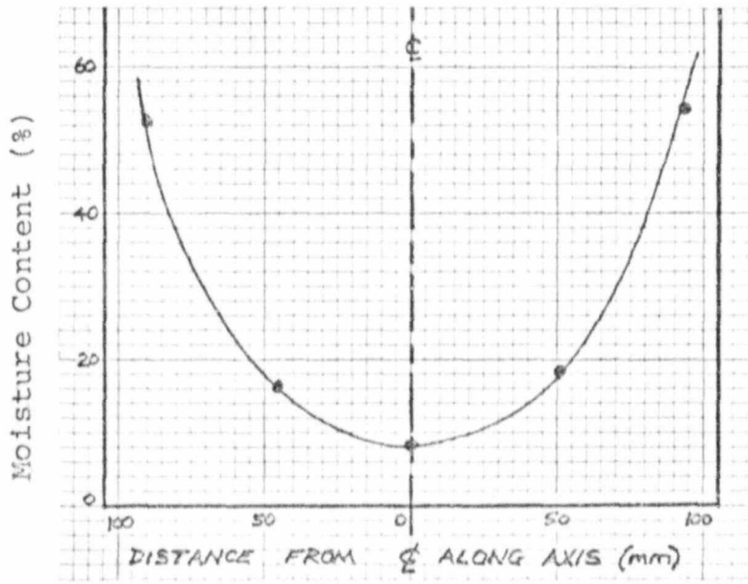


Fig. 20 Typical Moisture Content Profile (after loading to about 70 MPa)

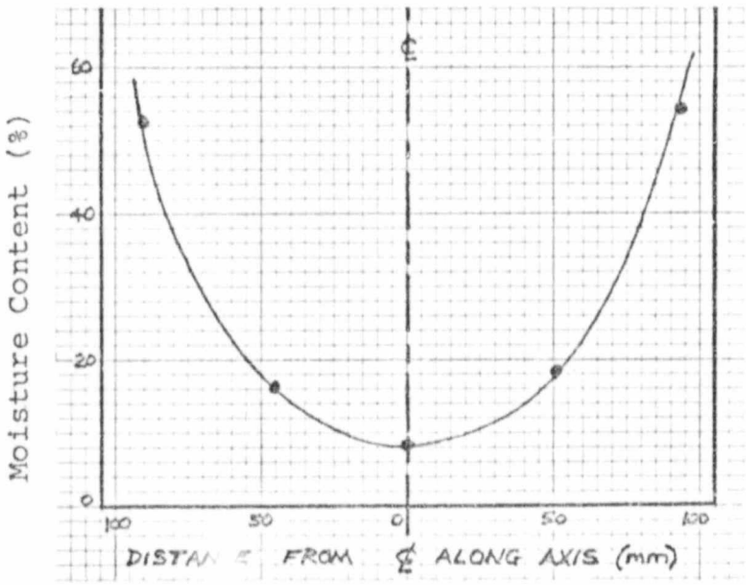


Fig. 20 Typical Moisture Content Profile (after loading to about 70 MPa)

(This is discussed further in 4.4 below). Stresses were again corrected by a constant factor relating area ratio after and before loading to closure strain. The tests were conducted on SGM slimes with 1:10 cement:slimes ratio and initially at 54% moisture content.

The first set of tests on reinforced slabs had all reinforcement at 30 mm spacing, and the effect of spanning the wires in one direction was compared with wires spanned in two directions. The results are shown in Fig. 21. The two-way spanned reinforced slab proved to be slightly superior to the one-way spanned and unreinforced slabs.

The effect of varying the spacing of the wires, or varying the area proportion of reinforcement in the slab, was also examined. Fig. 22 shows the results, and it is evident that due to the small proportions of reinforcement used, 0,12% to 0,48% by area, the effects of variations in spacing are not very marked although they are significant.

The improvement in strength development characteristics shown by the reinforced slabs over the unreinforced slab indicate that the wires were beneficial. The nature of this beneficial influence was further investigated in two tests on slabs of different plan dimensions reinforced in one direction only. Prior to casting, fine graduations were marked on the wires at set intervals. After the test, the graduated intervals were remeasured to record the plastic deformation that had occurred during compression of the slab.

The first slab was 180x180 mm in plan (height:side ratio 1:6) and it was reinforced in one direction only by wires at 30 mm centres. The wires were marked with fine graduations at 20 mm intervals. After loading the slab to about 80 MPa, the wires were removed and the graduated distances were measured for signs of plastic deformation. Fig. 23a shows the layout of the slab, and

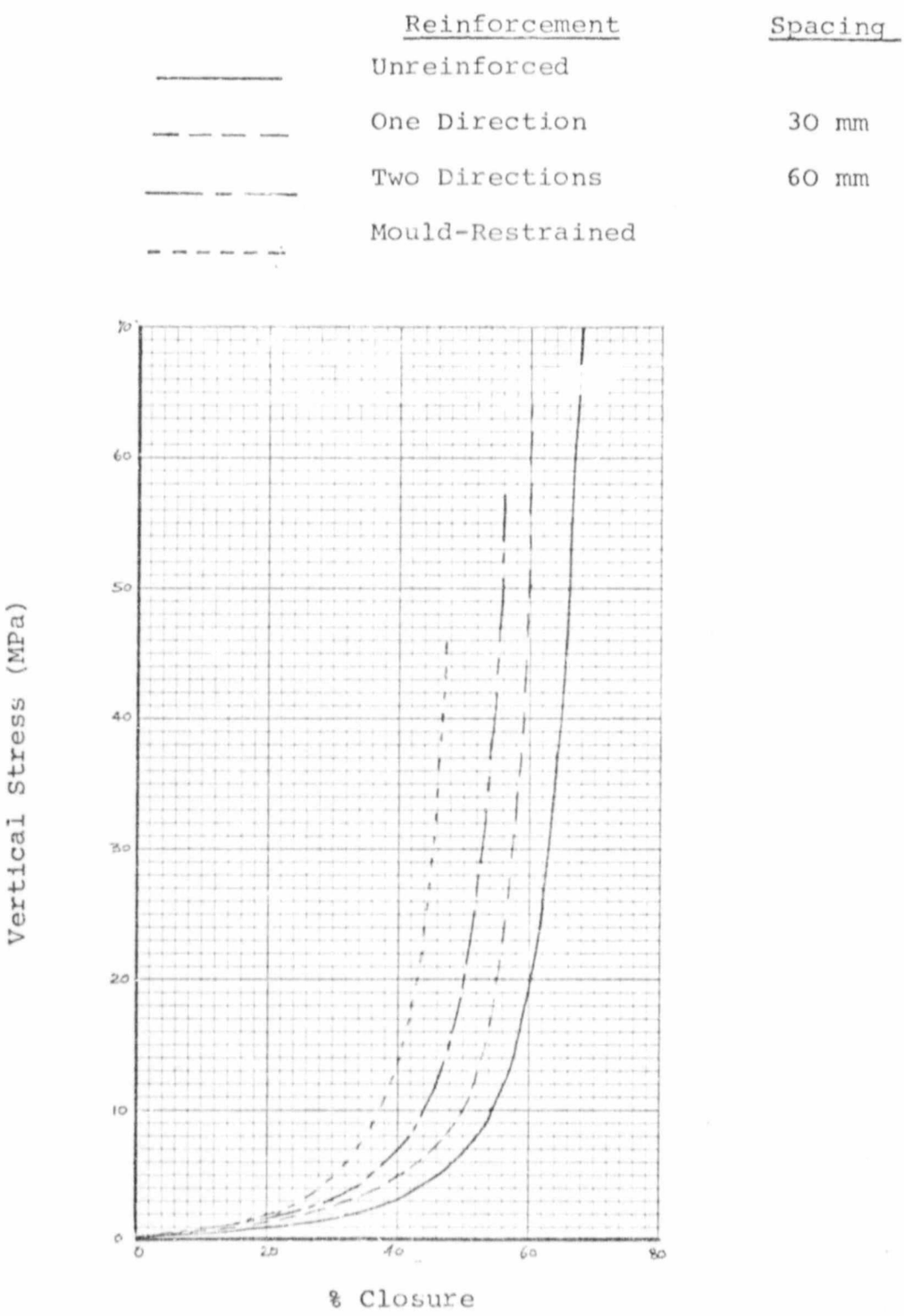


Fig. 21 Effect of One-and Two-Directional Reinforcement on Strength Development

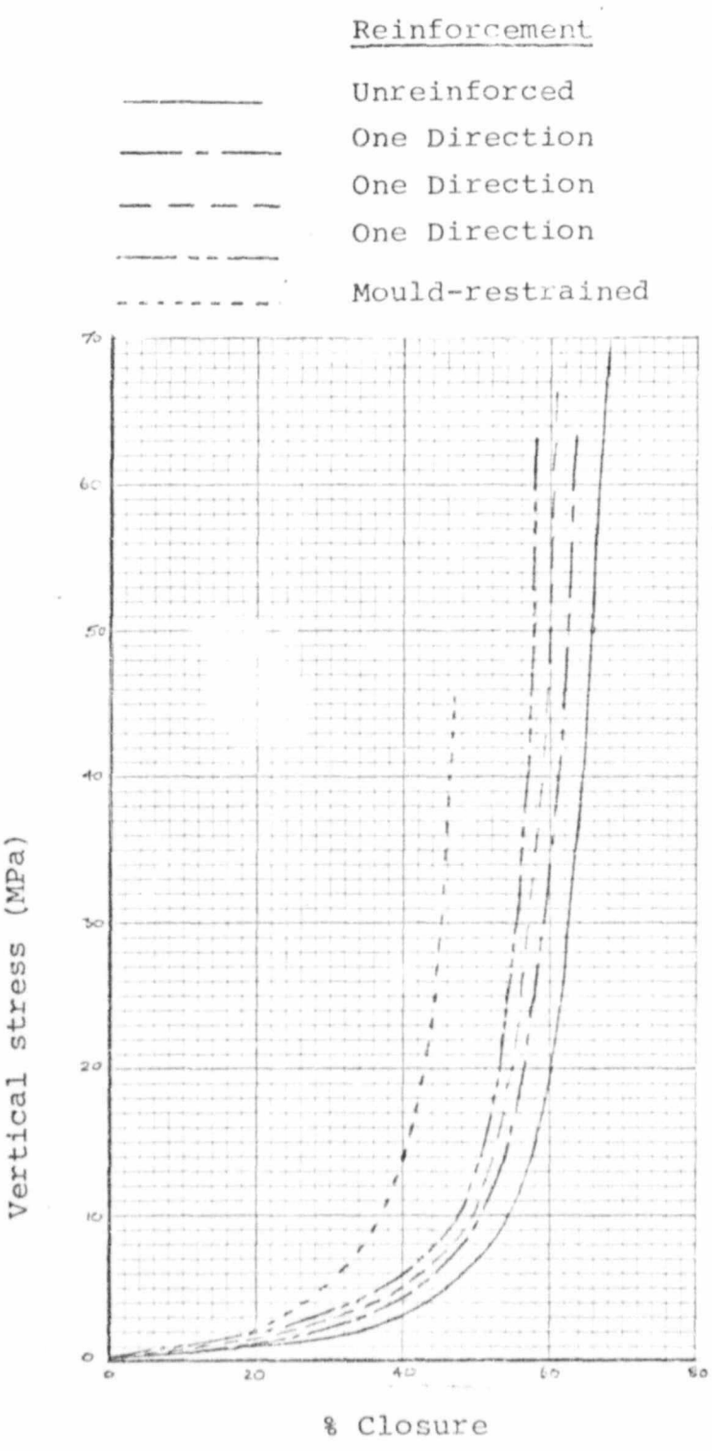


Fig. 22 Effect of Reinforcement Spacing on Strength Development (SGM slimes, 1:10 cement:slimes)

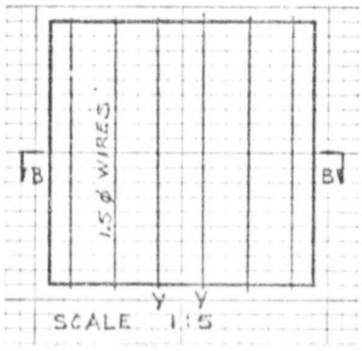


Fig. 23a Plan on Slab

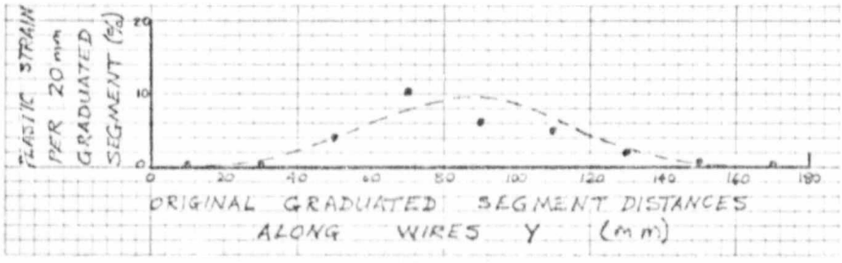


Fig. 23b Average plastic strain along wires Y after loading to 80 MPa

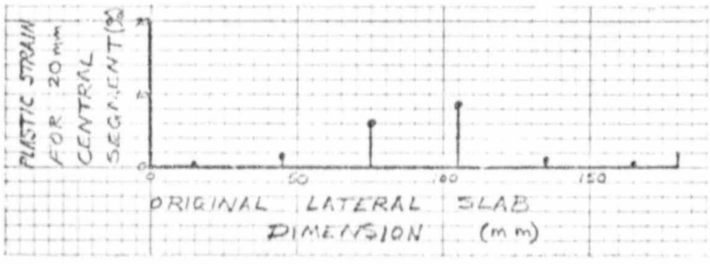


Fig. 23c Central plastic strain of wires across section B-B after loading to 80 MPa

Fig. 23 Monitored Plastic Deformations in Wires in a 180x180 mm Slab

Figs. 23b and 23c show the residual plastic deformations across both central axes of the slab. The percentage strains are calculated per graduated distance. The fact that considerable yield did occur is that a strong bond developed between the slimes mix and the wires. However, it was considered necessary to conduct a further test on a reinforced slab, and to mark graduations on the wires at closer intervals in order to better observe the onset of plastic deformation.

The second slab was 150x90 mm (height:shorter side ratio 1:3) and the wires, graduated at 10 mm intervals, were spanned across the shorter span and spaced at 30 mm centres. Fig. 24 shows the layout and gives the measured plastic deformations which were calculated as a percentage per graduated distance. Once again, sufficient bond was developed under load to cause the central wires to extend plastically.

From Figs. 23b and 24b, it is seen that lengths of wire remained unyielded at the ends of the central wires. In the cases of both the slabs, this length was about 15 mm, and it seems reasonable to assume that this is the upper limit to the bond length required for full shear bond between the wires and the slimes.

4.4 Mould-restrained Slabs

In order to assess the influence of lateral restraint on a slab, a slab with a mix ratio of 1:10 cement:SGM slimes was cast in a mild steel mould with 1 mm thick walls. Electric resistance strain gauges were glued to the mould at the centre of each side in order to monitor the lateral strains in the mould walls. The slab was initially 150x120 mm in plan, and due to the restraining influence of the mould, the slab effectively did not increase in area during the test.

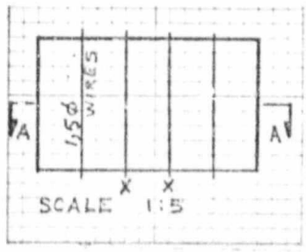


Fig. 24a Plan on Slab

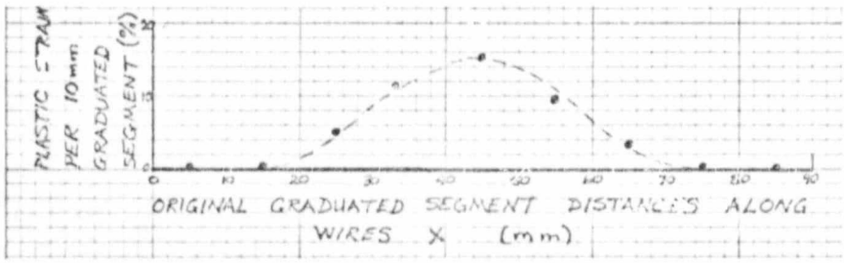


Fig. 24b Average plastic strain along wires X after loading to 80 MPa

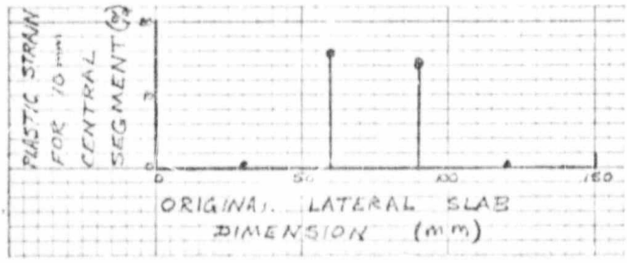


Fig. 24c Central plastic strain of wires across section A-A after loading to 80 MPa

Fig. 24 Monitored Plastic Deformations in Wires in a 150x90 mm Slab

Fig. 25a shows the stress-strain curve for the mould-restrained slab compared with a similar unrestrained slab. The improvement in strength development characteristics in the case of the mould-restrained slab is seen to be very large.

Fig. 25b is a plot of the closure or vertical strain versus the average lateral strains measured in the opposite pairs of strain gauges. The yield strain for mild steel is about 1 200 με, and this is seen to be exceeded at an early stage. The curve in Fig. 25b indicates a relationship of about 100:1 between the vertical and lateral strains. The lateral strain is thus insignificant compared with the vertical strain and the material is hence undergoing an essentially K_o consolidation, i.e. consolidation without significant lateral yield.

Once the beneficial effect of lateral restraint on strength development had been realised from the above results, three further tests on mould-restrained slabs were conducted. Two unstabilised slabs,one of SGM slimes and the other of ROD slimes, were tested for the effect of stabilising agents compared with lateral restraint. The third was a slab of ROD slimes with a 1:10 cement:slimes ratio.

The results of all tests on mould-restrained slabs compared with an unrestrained slab with 1:10 cement: SGM slimes are shown in Fig. 26. The general conclusion drawn from these curves is that the stabilising agent, which has a beneficial effect on the shear strength properties of the slimes, also has a beneficial effect on the strength development characteristics of slabs even when full lateral restraint is applied to the slabs. The beneficial effect of improved shear strength properties is further illustrated by comparing the curves of the two unstabilised slabs of SGM and ROD slimes, although the benefit is exaggerated due to the reduced moisture content in the ROD slimes.

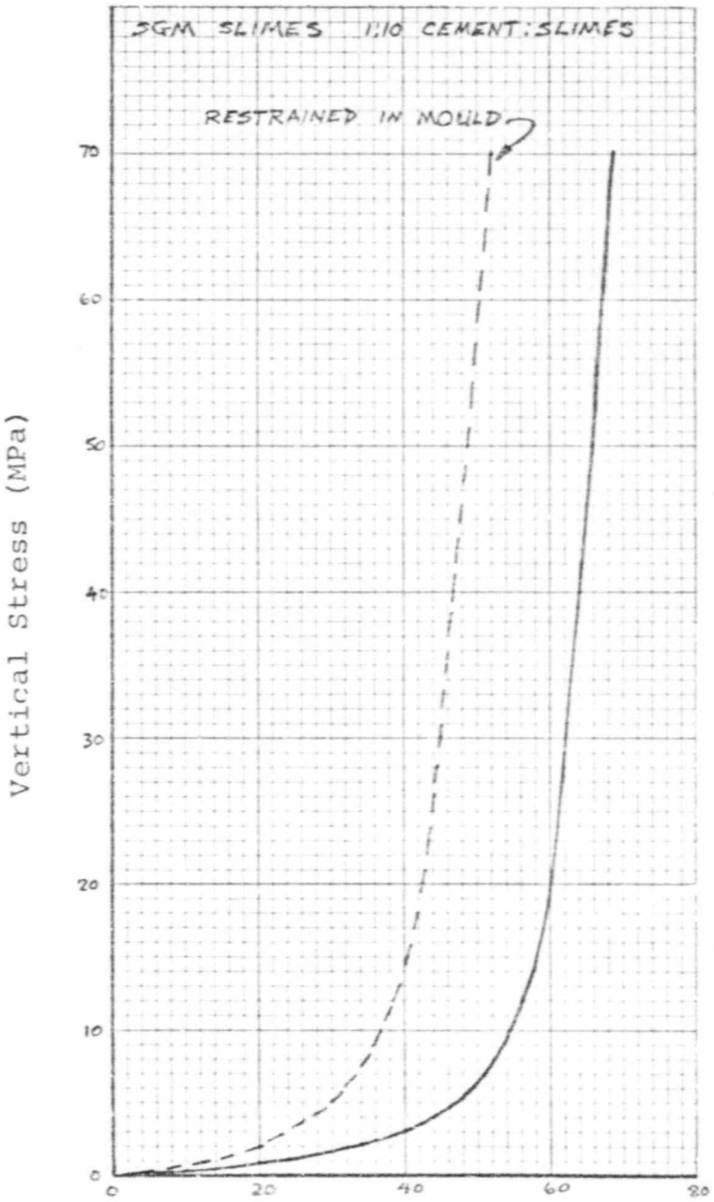


Fig. 25a Stress-Strain Curve

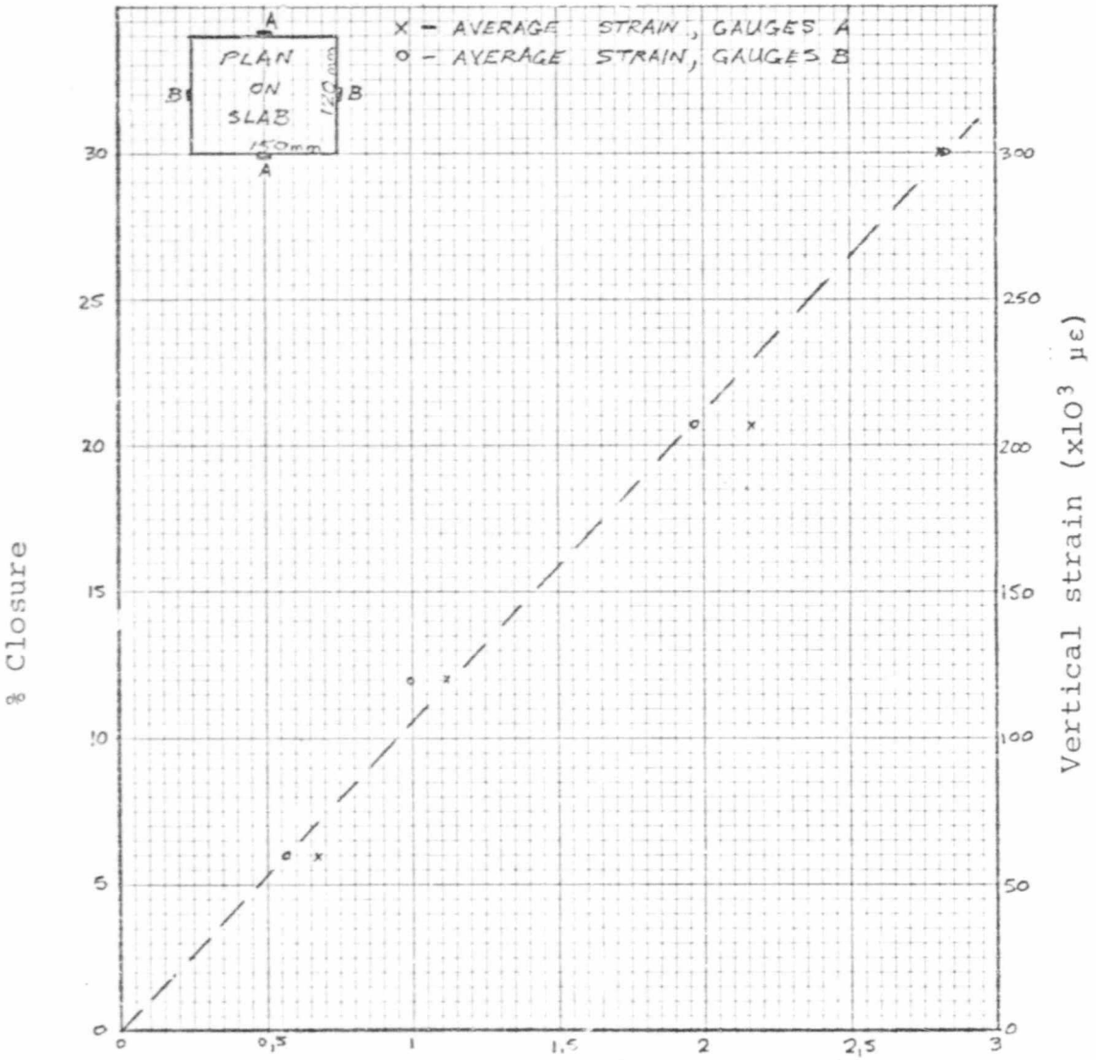


Fig. 25b Vertical-Lateral Strain Relationship

Fig. 25 Effect of Mould-restraint on Strength Development

	Slimes	Restraint	Cementing Agent
——— - ———	SGM	Mould-Restrained	Unstabilised
————————	SGM	Unrestrained	1:10 Cement: slimes
— — — — —	SGM	Mould-restrained	1:10 Cement: slimes
——— - - ———	ROD	Mould-restrained	Unstabilised
- - - - - - - -	ROD	Mould-Restrained	1:10 Cement: slimes

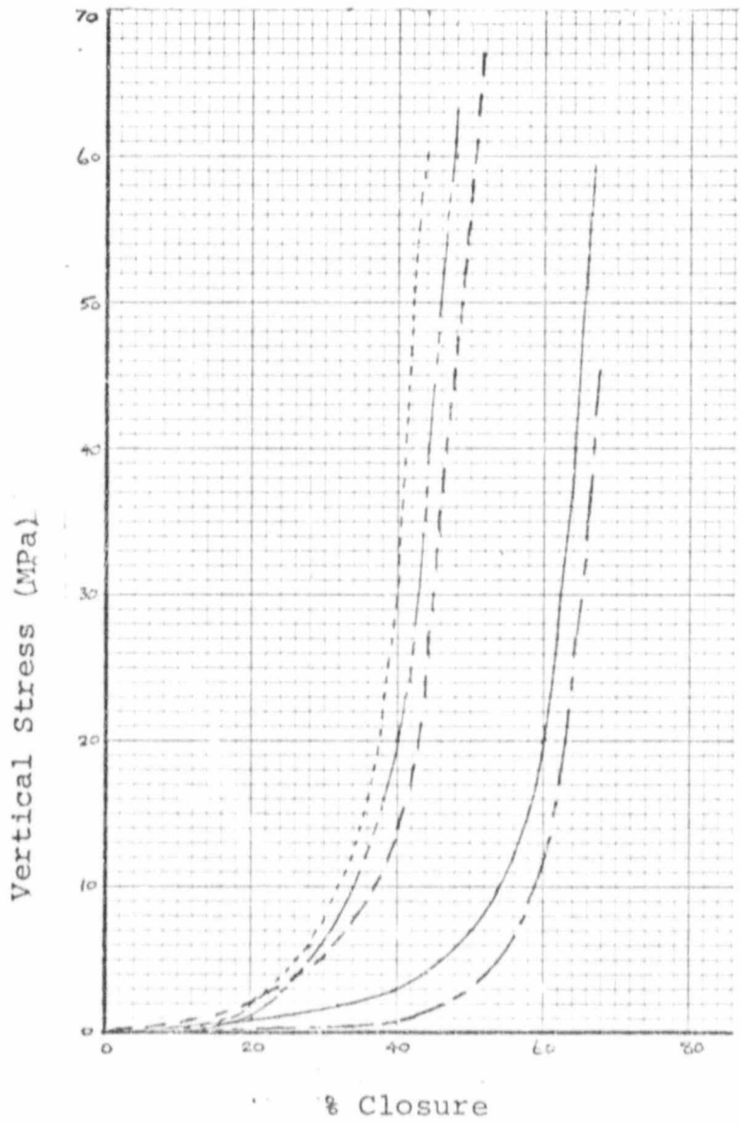


Fig. 26 Effect of Mould-Restraint and Cementing Agent on Strength Development

The effects of lateral restrain are summarized by plotting the area and A_f/A_i, where A_f = the final area and A_i = the initial area, versus the vertical stress at a particular percentage closure. Apart from the mould-restrained test, all slab compressions were accompanied by lateral movements of the material. The area ratio is calculated from the measured slab dimensions after and before testing. The curves in Fig. 27 are plotted for tests on stabilised slabs of SGM slimes. The vertical strengths were measured at 40% closure (Fig. 27a) and at 60% closure (Fig. 27b). The trend in the curves is quite apparent, variations from the smooth curve probably being due to the differing effects on shear properties of the various cementing agents. At 40% closure, the fully restrained slab (A_f/A_i = 1,0) could support a loading of approximately 14 MPa, but its strength development after this stage was so rapid that a closure of 60% could not be obtained within the capacity of the testing apparatus. The curtailment of lateral expansion of a slab is therefore beneficial to its strength development properties.

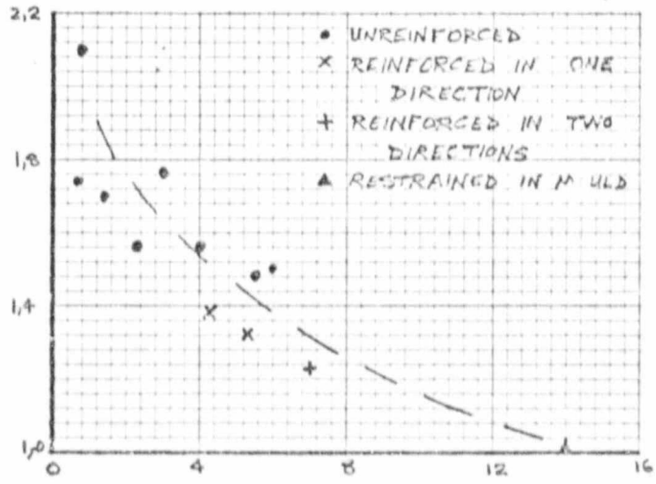
4.5 Theoretical Considerations

The tests on slab specimens were conducted in order to simulate conditions of closure on fill material in mining stopes. A theoretical consideration of the behaviour of the slabs is useful in scaling up the results of the laboratory tests to the field condition.

Two main problem areas are evident in the considerations of scaling. They are:

(i) the distribution of stress in the slabs, and

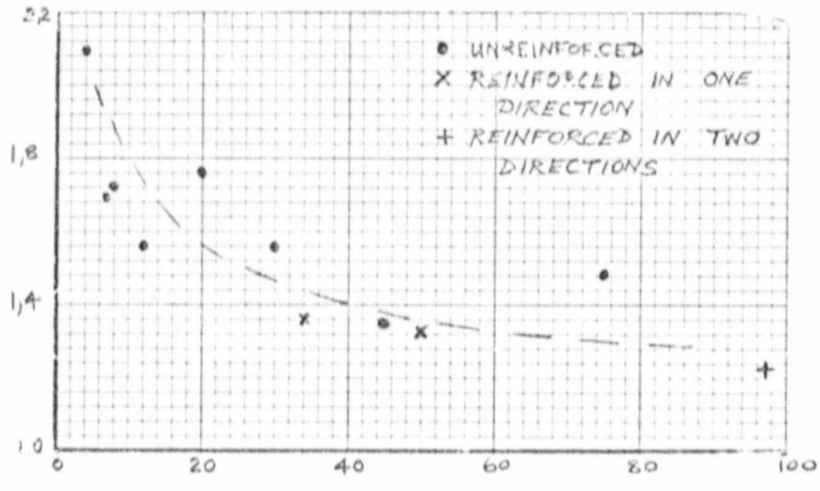
(ii) the drainage of water from the material.



Area Ratio Af/Ai

Vertical stress (MPa)

Fig. 27a At 4% Ciosure



Area Ratio Af/Ai

Vertical stress (MPa)

Fig. 27b At 60% Closure

Fig. 27 Effect of Lateral Restraint on Strength at Specified Closure

4.5.1 Stress Distribution

The compression tests on unreinforced slabs can be roughly represented as the plane flow of a ductile material compressed between flat surfaces, the planes $y = \pm a$. Assuming the planes to be rough and the material slipping over them to the right, the stress distribution depicted in Fig. 28 can be derived[13]. In calculating the stress distribution the Tresca yield criterion was assumed to apply, though this is not an accurate representation of the failure criterion for the slimes which has a friction-dependent shear strength.

The moisture content profile across the slab (see Fig. 20) and the distribution of plastic deformation in reinforcement wires (see Figs. 23 and 24) must be related in some way to the distribution of vertical stress across the slab. If it is assumed that the stress distribution is bell-shaped as in the moisture content profile and the plastic deformation distributions, then it can readily be seen that a straight line distribution of vertical stress as derived and shown in Fig. 28 will not give a very realistic or accurate representation of the field conditions. The cause of the discrepancy between the curves is probably the assumption that the Tresca yield criterion applies. The development of this theory to accurately represent the problem situation should be considered for further research.

Considering the bond information obtained from the tests on wire-reinforced slabs, it is possible to estimate the vertical stress in the slab at the onset of yield in the wire reinforcement. Fig. 29 shows a length of reinforcing wire of diameter d, which is yielding at a tensile force of $\sigma_y A_s$, where σ_y = the yield stress of the wire, due to a shear stress τ. τ acts normal to the vertical stress on the slab, σ_v, and if L_{max} is the maximum bond length, τ is assumed to vary linearly from zero to full value over L_{max}. Thus, for equilibrium of forces:

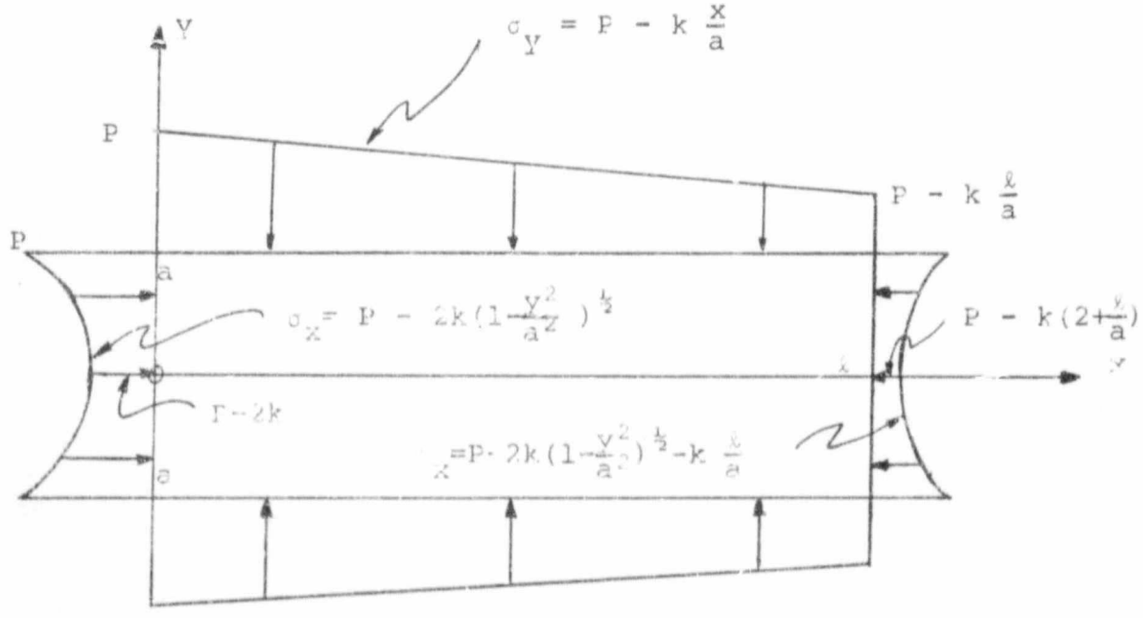


Fig. 28 Stress Distribution for Ductile Flow Between Two Planes[13]

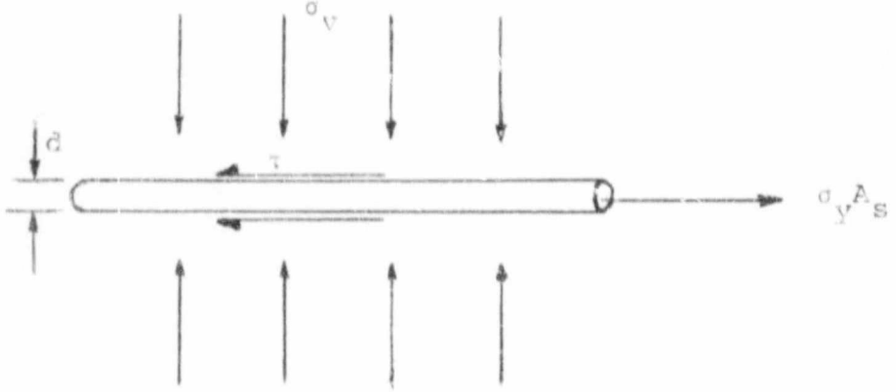


Fig. 29 Reinforcement Wire Yielding in Tension

$$\frac{\tau}{2} \pi d L_{max} = \sigma_y A_s \quad (1)$$

Also, τ is related to σ_v by Coulomb's equation:

$$\tau = C + \sigma_v \tan \phi \quad (2)$$

From equation (1):

$$\tau = \frac{2\sigma_y A_s}{\pi d L_{max}} \quad (3)$$

and from equations (2) and (3):

$$\sigma_v = \frac{2\sigma_y A_s}{\pi d L_{max} \tan\phi} - \frac{c}{\tan\phi} \quad (4)$$

For the 1:10 cement, SGM slimes mix, from Fig. 15, $c \approx 0$ and $\phi \approx 31^{\circ}$. For the wire σ_y can be taken as 250 MPa and d = 1,65 mm. From the results in 4.3 above, L_{max} = 15 mm. Thus, solving equations (3) and (4) gives:

$$\underline{\tau = 14 \text{ MPa}}$$

which corresponds to a value of

$$\underline{\sigma_v = 23 \text{ MPa}}$$

Noting that the slabs were tested to an average vertical stress of approximately 70 MPa, and concluding from the above calculation that the wires yield at a shear stress of about 14 MPa corresponding to a vertical stress on the slab of about 23 MPa, there are a number of conclusions that can be drawn from these results:

The yielding wires can support no more than a 23 MPa vertical stress, which means that once the vertical stress on the slab exceeds 23 MPa the wires actually have a weakening effect on the material in their immediate vicinity. However, the results of the first sets of wire-reinforced slab tests (see Figs. 21 and 22) indicate that the wires do improve the strength development characteristics of

the slab. It is probable therefore that the wires benefit the slab in two ways

a) they assist in improving the initial load-bearing ability until they yield, and

b) they assist towards the edges of the slab where vertical stresses are lower than 23 MPa.

Following from the above discussion, it seems worth noting that although an increase in the area proportion of the wire might improve the initial strength development, the increased weakening effect at higher vertical stresses might be significantly detrimental to strength development at later stages. There is probably an optimum amount of reinforcement where beneficial assistance reaches a limit before detrimental effects govern.

Considering now the mould-restrained slabs, it is possible to obtain an indication of the magnitudes of horizontal stresses in a slab. Results have shown that the steel in the mould walls does yield (see Fig. 25b) and horizontal pressures can thus be calculated at onset of yield. If the mild steel mould is assumed to be equivalent to a hoop of thickness t, containing a cylinder of material of diameter d, under a pressure p, then at onset of yield in the steel, the hoop stress σ_h is equal to the yield stress σ_y:

$$\sigma_h = \frac{pd}{2t} = \sigma_y \qquad (5)$$

or

$$p = \frac{2t\sigma_y}{d} \qquad (6)$$

As an estimation of d, either the area of the slab or its perimeter can be taken as equivalent to the assumed cylinder. If the plan dimensions of the slab are lxb, then, in terms of equivalent areas:

$$\frac{\pi d^2}{4} = lb$$

$$\text{or} \quad d = \frac{2}{\pi}(\pi lb)^{\frac{1}{2}} \qquad (7)$$

and in terms of equivalent perimeters:

$$\pi d = 2(l+b)$$

$$\text{or} \quad d = \frac{2}{\pi}(l+b) \qquad (8)$$

For the 150x120 mm slab as tested, equation (7) gives:

$$d = 151 \text{ mm} \qquad (9)$$

and equation (8) gives:

$$d = 172 \text{ mm} \qquad (10)$$

Taking t = 1 mm and σ_y = 250 MPa, equations (6) and (9) give:

$$p = 3{,}3 \text{ MPa}$$

and equations (6) and (10) give:

$$p = 2{,}9 \text{ MPa}$$

Thus, p, the horizontal stress in the slimes mix, was approximately 3 MPa at onset of yield in the mould walls. Working from Fig. 25b to Fig. 25a, obtaining the % closure (12,5%) at onset of yield (1 200 με), the average vertical stress on the slab is seen to be approximately 1 MPa. It is thus seen that small vertical stresses (3 MPa = 30 atmospheres ≈ 150m(of overburden)which are required to substantially improve strength development. It was concluded in 4.4 that consolidation took place without significant lateral yield in the mould walls, which shows that the high strength of the mould steel provides full restraint against substantial lateral pressures in the slab.

4.5.2 Drainage

Strength has been shown to increase with reducing moisture content (see Fig. 19) and it is thus of value to consider the drainage of water from the material. A heat flow analogy can be adapted to describe the flow of water out of the material under load, as was done by Blight[12] using Carslaw and Jaeger[14] to obtain a solution to the differential equation describing the consolidation of soil in the vicinity of a shear vane. A number of assumptions relating to excess pore pressures would have to be made in order to carry out the analysis, which is considered to fall outside the scope of this dissertation.

5. LIQUEFACTION STUDIES

The problem of liquefaction mentioned in Chapter 1 will now be investigated. The test method involved cyclic loading triaxial tests, drained and undrained, conducted on isotropically consolidated specimens of both SGM and ROD slimes mixes with 1:10 cement:slimes ratios. In the drained tests, pore water pressures were monitored. The load in each cycle was increased to about half the failure load (taken from the static loading triaxial test results) and then reduced to zero, the rate of strain being kept approximately constant. The total time for each loading and unloading cycle was about 15 minutes.

Fig. 30 shows the plots of volume change and pore water pressure against the number of repetitions of the loading cycle, and Fig. 31 shows axial strain versus number of repetitions.

Liquefaction failure occurs when the pore water pressure builds up to become equal to the confining pressure[10], and, considering this fact, various inferences can be drawn from the results shown in Fig. 30 and 31. The rising pore water pressure curves indicate a situation where liquefaction might occur. The evidence of stronger dilatancies shown by the ROD slimes in the static loading triaxial tests (see 3.2 and Fig. 14) is to some degree contradicted by the curves in Fig. 30, although the pore pressure build-up is much lower than with the SGM slimes and is considerably less than the confining pressure.

The curves in Fig. 31 tend more to the horizontal than the curves in Fig. 30. This stabilising tendency indicates a densification which may counter factors leading to liquefaction, especially considering that axial strain has been observed to increase rapidly at liquefaction[10].

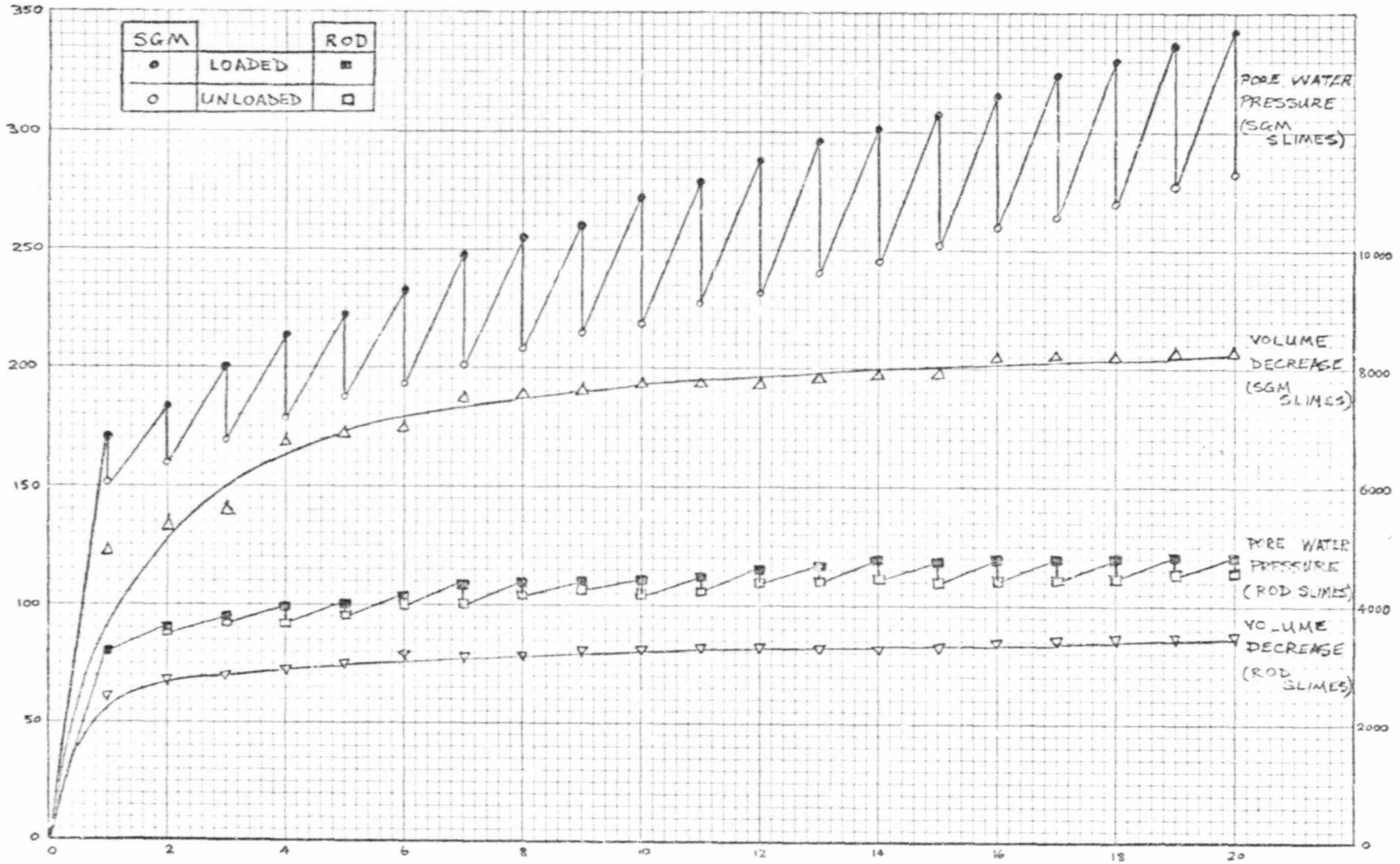


Fig. 30 Pore Water Pressure and Volume Decrease Cruves during Cyclic Loading
(1:10 Cement:slimes ratio, 7-11 days curing period,
Cell Pressure = 493 kPa, Consolidation Pore Pressure = Atmospheric)

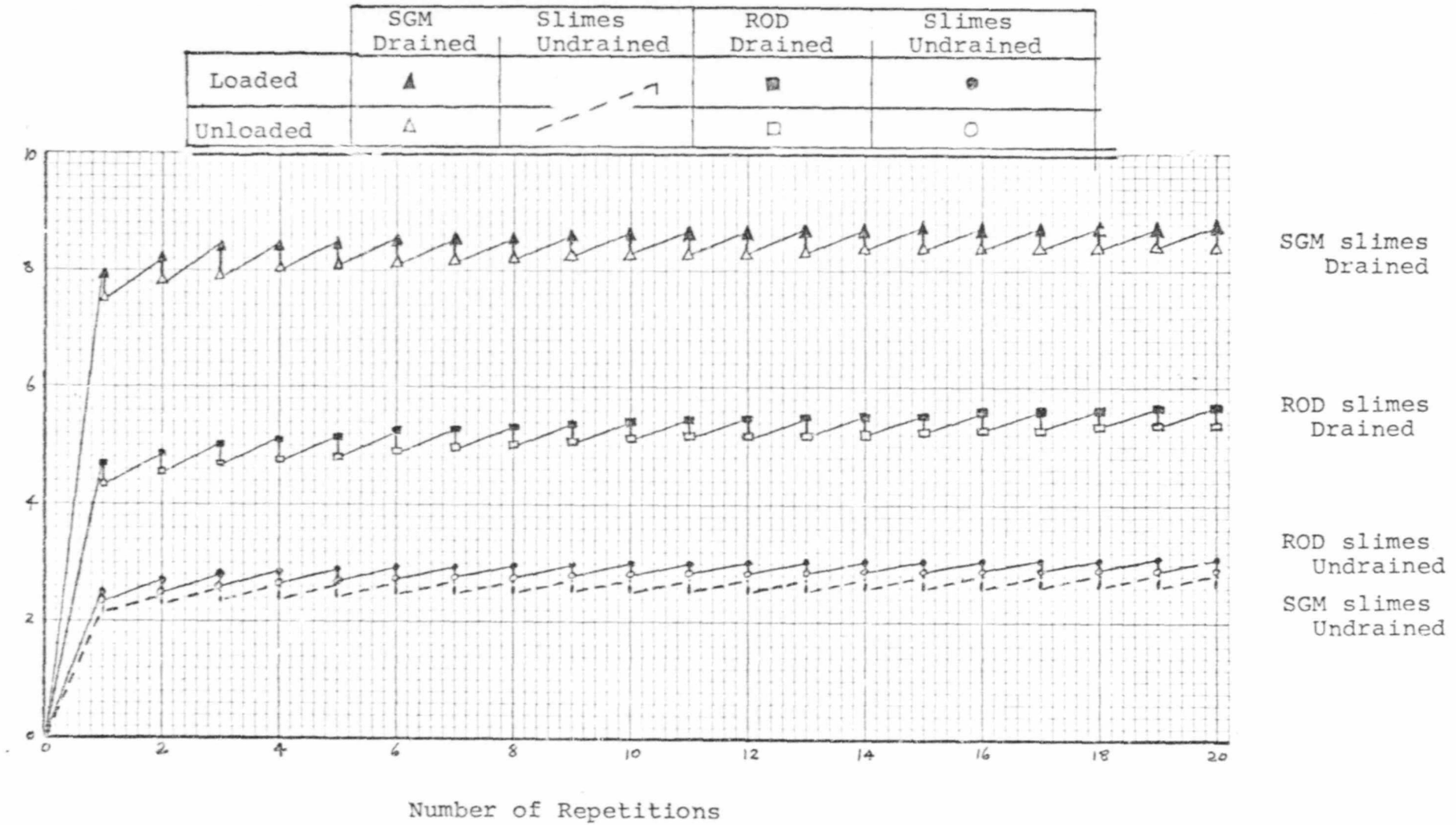


Fig. 31 Axial Strain Curves during Cyclic Loading
(1:10 Cement:slimes Ratio, 7-11 days curing period,
Cell Pressure = 493 kPa, Consolidation Pore Pressure = Atmospheric)

Author Avalle Derek Luigi
Name of thesis Properties Of Weakly Cemented Slurries Of Gold Mine Slimes. 1976

PUBLISHER:

University of the Witwatersrand, Johannesburg
©2013

LEGAL NOTICES:

Copyright Notice: All materials on the University of the Witwatersrand, Johannesburg Library website are protected by South African copyright law and may not be distributed, transmitted, displayed, or otherwise published in any format, without the prior written permission of the copyright owner.

Disclaimer and Terms of Use: Provided that you maintain all copyright and other notices contained therein, you may download material (one machine readable copy and one print copy per page) for your personal and/or educational non-commercial use only.

The University of the Witwatersrand, Johannesburg, is not responsible for any errors or omissions and excludes any and all liability for any errors in or omissions from the information on the Library website.